

General relativistic compact stars with exotic matter

N. Yasutake*, T. Maruyama[†], T. Tatsumi**, K. Kiuchi[‡] and K. Kotake*

**Division of Theoretical Astronomy, National Astronomical Observatory of Japan, 2-21-1 Osawa, Mitaka, Tokyo 181-8588, Japan*

[†]*Advanced Science Research Center, Japan Atomic Energy Agency, Tokai, Ibaraki 319-1195, Japan*

***Department of Physics, Kyoto University, Kyoto 606-8502, Japan*

[‡]*Department of Physics, Waseda University, 3-4-1 Okubo, Shinjuku-ku, Tokyo 169-8555, Japan*

Abstract. We study structures of general relativistic compact stars with exotic matter. Our study is based on axisymmetric and stationary formalism including purely toroidal magnetic field. We also study the finite size effects of quark-hadron mixed phase on structures of magnetars. For hybrid stars, we find a characteristic distribution of magnetic field, which has a discontinuity originated in the quark-hadron mixed phase. These distributions of magnetic field will change astrophysical phenomena, such as cooling processes.

Keywords: Neutron stars

PACS: 97.60.Jd; 26.60.-c

INTRODUCTION

It was presented that quark matter may exist in compact stars [1, 2, 3]. So far, there has been extensive work devoted to studying the effects of quark matter on astrophysical phenomena; the gravitational wave radiation [4, 5, 6], cooling processes [7, 8, 9, 10], neutrino emissions [11, 12], and rotational frequencies [13], the maximum energy release by conversions from neutron stars to quark/hybrid stars [14, 15], etc.. However, uncertainties of equation of states (EOSs) have been still left.

For such studies on compact stars, general relativistic effects are fundamentally important, since baryon density is comparable to pressure, $\rho_0 c^2 \sim P$, hence the gravitational force is strong. Moreover, strong magnetic field may change hydrostatic equilibriums of compact stars.

In this paper, we study the structures of general relativistic hybrid stars with purely toroidal magnetic field. To calculate magnetized compact stars, we adopt the scheme based on axisymmetric and stationary formalism including purely toroidal magnetic field [16]. A star with pure toroidal magnetic field is unstable, however it becomes another stable star in which toroidal magnetic field is dominant in the dynamical simulation [17]. Moreover, Heger et al. have suggest that the toroidal magnetic field may dominate 10^5 times larger than the poloidal magnetic field at the last stage of the main sequence [18].

The organization of this paper is as follows. Adopted EOSs are briefly discussed in Sec. 2 with equilibriums of magnetized rotating compact stars. In Sec. 3, we show our numerical results. In Sec. 4, we discuss the consequence of our calculations.

INPUT PHYSICS

Equation of state

The hardness of EOSs is an important ingredient for determining the equilibrium configurations as mentioned in Sec. 1. Though proto-neutron stars left after supernova explosions are very hot, $T \sim 50$ MeV, they cool down to cold neutron stars ($T \sim 1$ MeV) in some tens of seconds [19]. Therefore we assume that the temperature for hydrostatic compact stars is zero, since EOSs at such low temperature ($T \sim 1$ MeV) show almost same stiffness as at zero-temperature. It means the temperature of compact stars is always much smaller than the typical chemical potentials. Moreover, the loss of neutrinos means that the chemical potentials of the neutrinos may be set to zero. Thus, we impose the barotropic condition of the EOSs ($P = P(\epsilon)$) by assuming zero-temperature, zero-neutrino fraction, and beta-equilibrium.

Our theoretical framework for the hadronic phase of matter is the nonrelativistic Brueckner-Hartree-Fock approach including hyperons such as Σ^- and Λ [20].

For quark phase, we adopt the MIT bag model for quark phase of u , d , s -quarks, because this is the first step for the study on structures of hybrid stars with rotation and magnetic field in the general relativistic formulations, though it is a toy model. We use massless u and d quarks, and s -quark with a current mass of $m_s = 180$ MeV. We set that the bag constants, B , is 100 MeV fm^{-3} in this paper. Values of $B > 150 \text{ MeV fm}^{-3}$ can also be excluded within our model, because we do not obtain any more a phase transition in beta-stable matter in combination with our hadronic EOS.

For mixed phase, we must take into account the Gibbs condition, which require the pressure balance and the equality of the chemical potentials between the two phases besides the thermal equilibrium [21]. We use the Thomas-Fermi-approximation for the density profiles of hadrons and quarks. In each cell, we must calculate the balance of the colomb interaction and the surface tension. However, there are a wide range of uncertainties about the surface tension, $\sigma \sim 10 - 100 \text{ MeV fm}^{-2}$, which are suggested by some theoretical estimates based on the MIT bag model for strangelets [22] and lattice guage simulations at finite temperature [23, 24].

As for this uncertainty, Maruyama et al. have showed that the surface tensions of $\sigma > 40 \text{ MeV fm}^{-2}$ do not change the hardness of EOSs [25]. Then, we adapt two values of surface tension as $\sigma = 10 \text{ MeV fm}^{-2}$ for the minimum case, and $\sigma = 40 \text{ MeV fm}^{-2}$ for the maximum case.

At the maximum densities higher than two times of saturation density, muons may appear[26, 27]. However, we neglect it, since the muon contribution to pressure at the higher density has been pointed to be very small [28].

Finally, we show our EOSs on Fig. 1. The left two panels show the pressure versus the baryon density for the quark-hadron mixed phase. For weak surface tension ($\sigma = 10 \text{ MeV fm}^{-2}$), the droplet structure does not appear, whereas, for strong surface tension ($\sigma = 40 \text{ MeV fm}^{-2}$), the rod structure does not appear. The number of hyperons are suppressed because of the appearance of quarks for both surface tensions. The right panel is for EOSs of nuclei with/without hyperons.

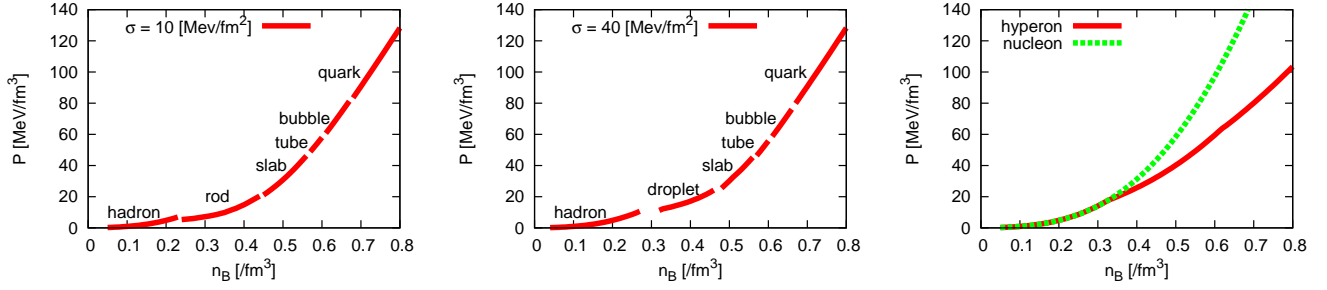


FIGURE 1. Baryon number density versus pressures for each matter. The left (center) panel is for an EOS with quark-hadron mixed phase under $B=100 \text{ MeV fm}^{-3}$ and $\sigma = 10$ (40) MeV fm^{-2} . The right panel is for hadronic EOSs with (without) hyperons shown as a solid (dashed) line. Here, we assume neutrino free and zero temperature for all cases; $Y_{\nu_e} = 0$, $T = 0$.

Equilibrium of magnetised rotating compact stars

Master equations for the rotating relativistic stars containing purely toroidal magnetic fields are based on the assumptions summarized as follows [16]; (1) Equilibrium models are stationary and axisymmetric. (2) The matter source is approximated by a perfect fluid with infinite conductivity. (3) There is no meridional flow of the matter. (4) The equation of state for the matter is barotropic. (5) Magnetic axis and rotation axis are aligned. This barotropic condition can be maintained for our EOSs.

NUMERICAL RESULTS

Now, we show the configurations of strongly magnetized compact stars with/without quark-hadron mixed phase. In this paper, we consider the no-rotating static configurations for the following two reasons. (1) Since the magnetars and the high field neutron stars observed so far are all slow rotators, the static models could well approximate to such stars. (2) In the static models, one can see purely magnetic effects on the equilibrium properties because there is no centrifugal force and all the stellar deformation is attributed to the magnetic stress. In Fig. 2 and Fig. 3, we show distributions of the baryon density and the magnetic field in the meridional planes for the two static equilibrium stars characterized by (1) $\rho_{0,c} = 1.58 \times 10^{15} [\text{g}/\text{cm}^3]$, $B_{max} = 6.2 \times 10^{17} \text{ G}$, $M = 1.31M_{\odot}$, $R_{cir} = 9.97\text{km}$, $H/|W| = 2.11 \times 10^{-3}$ with the quark-hadron phase transition ($\sigma = 40\text{MeV}/\text{fm}^2$) [Fig. 2] and by (2) $\rho_{0,c} = 2.56 \times 10^{15} [\text{g}/\text{cm}^3]$, $B_{max} = 7.1 \times 10^{17} \text{ G}$, $M = 1.31M_{\odot}$, $R_{cir} = 9.42\text{km}$, $H/|W| = 1.64 \times 10^{-3}$ of nucleon EOS with hyperons [Fig. 3]. Each physical value is as follows; the baryon mass density $\rho_{0,c}$, the gravitational mass M , the circumferential radius at the equator R_{cir} , the maximum strength of the magnetic fields B_{max} , the ratio of the magnetic energy to the gravitational energy $H/|W|$. These two models have a same magnetic flux of $5.00 \times 10^{29} \text{ G cm}^2$ and a same baryon mass of $1.45M_{\odot}$.

Clearly, the distributions of magnetic field are different. The toroidal magnetic field lines behave like a rubber belt that is wrapped around the waist of the stars with hyperon

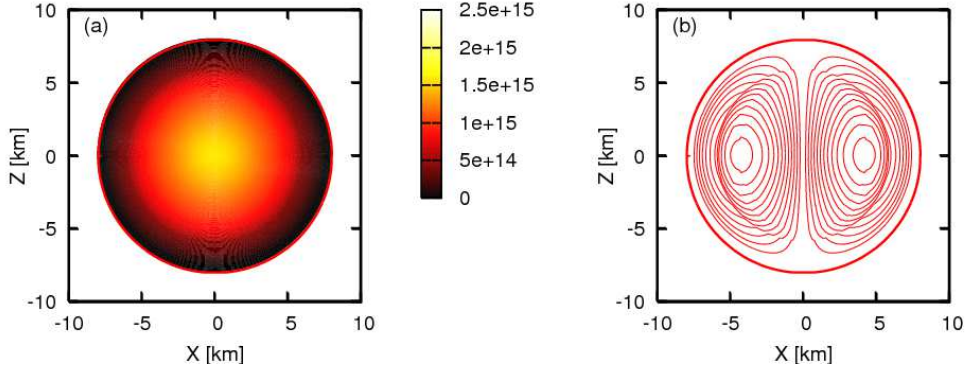


FIGURE 2. Distribution of (a): rest mass density [g/cm^3] and (b): magnetic field [G] with the quark-hadron phase transition ($\sigma = 40 \text{ MeV}/\text{fm}^{-2}$).

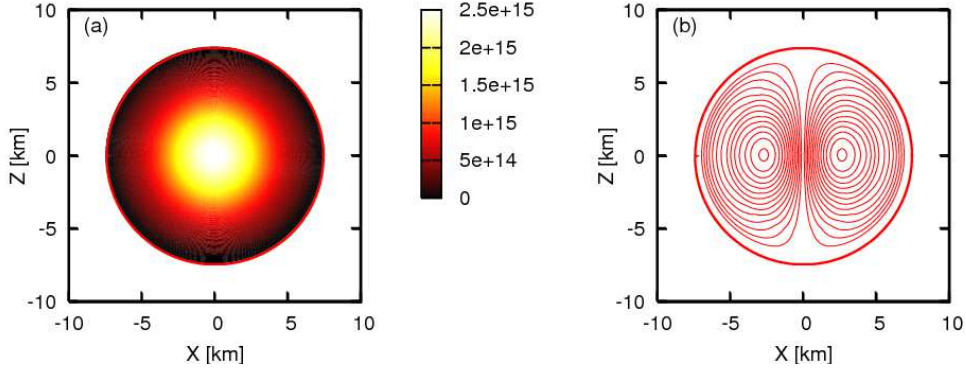


FIGURE 3. Same as FIG. 2 but without the phase transition.

EOS (see Fig. 3). However, for a hybrid star, the distribution of magnetic field has discontinuity for the equatorial direction (see Fig. 2). We can understand this easily; The magnetic field is frozen in the matter, hence the distribution of magnetic field depend on the distribution of the density. Hybrid stars have discontinuities of density profiles because of the phase transition; e.g. in FIG. 2, the 6 km from the core of a hybrid star is the mixed phase matter, and the baryon density in this density region has discontinuity, which raise the discontinuity of magnetic field as shown in the right panel of Fig. 2.

SUMMARY AND DISCUSSION

In this study, we have investigated the effects of quark-hadron mixed phase on the magnetized rotating stars of the general relativistic equilibrium configuration. As a result, we find that the distribution of magnetic field for hybrid stars has a discontinuity in the quark-hadron mixed phase.

Let us move on effects of strong magnetic field on EOSs. It was pointed out that the strong magnetic field may change EOSs [29]. In their study, they estimate the critical strength of magnetic field which may change EOSs, $\sim 10^{18} \text{ G}$. In our study,

we calculate the structures of magnetized compact stars around 10^{18} G. Hence, such magnetic field may change EOSs. Especially for quark matter, it has founded that the energy gaps of magnetic Color-Flavor-Locked phase are oscillating functions of the magnetic field [30, 31]. Their effects are also important, and may change our results.

As for the temperature and lepton fraction, we assume zero-temperature and neutron free. We will check our result under finite temperature and neutrino trapped cases. It will be useful for a study on structures of proto-compact stars, or may effect on cooling process and cooling curves of compact stars.

ACKNOWLEDGMENTS

We thank Y. Eriguchi, S. Yoshida for informative discussions.

REFERENCES

1. N. Itoh, *PTP* **44**, 291 (1970).
2. A. R. Bodmer, *PRD* **4**, 160 (1971).
3. E. Witten, *PDR* **30**, 272 (1984).
4. L. M. Lin, K. S. Cheng, M. C. Chu, and W. M. Suen, *ApJ* **639**, 382 (2006).
5. N. Yasutake, K. Kotake, M. Hashimoto, and S. Yamada, *PDR* **75**, 084012 (2007).
6. E. B. Abdikamalov, H. Dimmelmeier, L. Rezzolla, and J. C. Miller, *astro-ph/0806*, 1700 (2008).
7. D. Page, M. Prakash, J. M. Lattimer, and A. W. Steiner, *PRL* **85**, 2048 (2000).
8. D. Blaschke, T. Klahn, and D. N. Voskresensky, *ApJ* **533**, 406 (2000).
9. D. Blaschke, H. Grigorian, and D. Voskresensky, *A&A* **368**, 561 (2001).
10. H. Grigorian, D. Blaschke, and D. Voskresensky, *PRC* **71**, 045801 (2005).
11. K. Nakazato, K. Sumiyoshi, and S. Yamada, *PRD* **77**, 103006 (2008).
12. I. Sagert, M. Hempel, G. Pagliara, J. Schaffner-Bielich, T. Fischer, A. Mezzacappa, F. K. Thielemann, and M. Liebendörfer, *astro-ph/0809*, 4225 (2008).
13. G. F. Burgio, H. J. Schulze, and F. Weber, *A&A* **408**, 675 (2003).
14. N. Yasutake, M. Hashimoto, and Y. Eriguchi, *PTP* **113**, 953 (2005).
15. J. L. Zdunik, M. Bejger, P. Haensel, and E. Gourgoulhon, *A&A* **465**, 533 (2007).
16. K. Kiuchi, and S. Yoshida, *PRD* **78**, 044045 (2008).
17. K. Kiuchi, M. Shibata, and S. Yoshida, *astro-ph/0805*, 2712 (2008).
18. A. Heger, S. E. Woosley, and H. C. Spruit, *ApJ* **626**, 350 (2005).
19. A. Burrows, and J. M. Lattimer, *ApJ* **307**, 178 (1986).
20. M. Baldo, G. F. Burgio, and H.-J. Schulze, *PRC* **58**, 3688 (1998).
21. H. Heiselberg, C. J. Pethick, and E. F. Staubo, *PRL* **70**, 1355 (1993).
22. E. Farhi, and R. L. Jaffe, *PRD* **30**, 2379 (1984).
23. S. Huang, J. Potvion, C. Rebbi, and S. Sanielevici, *PRD* **42**, 2864 (1990).
24. K. Kajantie, L. Kärkäinen, and K. Rummukainen, *Nucl. Phys. B* **357**, 693 (1991).
25. T. Maruyama, S. Chiba, H.-J. Schulze, and T. Tatsumi, *PRD* **76**, 123015 (2007).
26. R. B. Wiringa, V. Filks, and A. Fabrocini, *PRC* **38**, 1010 (1988).
27. A. Akmal, V. R. Pandharipande, and D. G. Ravenhall, *PRC* **58**, 1804 (1998).
28. F. Douchin, and P. Haensel, *A&A* **380**, 151 (2001).
29. A. Broderick, M. Prakash, and J. M. Lattimer, *ApJ* **537**, 351 (2000).
30. J. L. Noronha, and I. A. Shovkoy, *PRD* **76**, 105030 (2007).
31. K. Fukushima, and H. J. Warringa, *PRD* **78**, 039902 (2008).